LWT - Food Science and Technology 250 (2026) 119443

Contents lists available at ScienceDirect

LWT

journal homepage: www.elsevier.com/locate/lwt

Multiscale characterization of plant protein-hydrocolloid soft-solids: Linking rheology, tribology, and mucoadhesion in texture-controlled formulations

Laura Piazza *, Giorgio Innocenzo Ascrizzi

Department of Environmental Science and Policy, Università degli Studi di Milano, 20133, Milan, Italy

ARTICLE INFO

Keywords:
Plant proteins
Weak gels
Soft tribology
Mucoadhesion
Texture engineering

ABSTRACT

Plant protein-hydrocolloid soft-solids exhibit coupled bulk and interfacial properties that cannot be described by steady shear viscosity alone. In this work, flaxseed- and hempseed-based formulations structured with carboxymethylcellulose, high-acyl gellan gum, or hydrolytic enzymes were investigated through a combined approach integrating steady and dynamic rheology, thixotropy, back extrusion, tribology, and ex-vivo mucoadhesion. Flow behavior was modelled using the Herschel-Bulkley equation, with yield stress ranging from 1.4 to 17.8 Pa and apparent viscosity at 50 s^{-1} from 0.7 to 2.9 Pa·s, highlighting the impact of structuring strategy on flow activation and low-shear resistance. Mechanical spectra revealed weak gel-like behavior (G' > G''), with formulation-dependent differences in network strength and frequency dependence. Structural recovery and large-deformation responses further differentiated protein-hydrocolloid interactions. Tribology revealed distinct boundary-to-hydrodynamic lubrication transitions and formulation-dependent friction coefficients. Ex-vivo mucoadhesion tests showed detachment forces between 0.03 and 0.5 N, evidencing interfacial retention mechanisms not predictable from bulk rheology alone. Hydrocolloid incorporation primary governed lubrication and adhesion under low shear conditions, whereas protein composition modulated network connectivity and recovery dynamics. Integrating yield stress, viscoelasticity, friction, and mucoadhesion enabled quantitative mapping of formulation-dependent performance, providing a structure-function framework for engineering of texture-controlled soft-solids with tunable mechanical and interfacial properties.

1. Introduction

Structured soft-solids based on plant proteins and hydrocolloids represent a rapidly expanding class of food systems, driven by increasing demand for plant-based formulations and texture-controlled products (Machado et al., 2025). Flaxseed and hempseed proteins are of particular interest due to their functional properties, including water-binding capacity, emulsification potential, and gel-forming ability (Chen et al., 2023; Lorenc et al., 2022). However, their structuring behavior strongly depends on interactions with hydrocolloids, which modulate network formation, phase organization, and mechanical response. Understanding these structure-function relationships is essential for rational formulation design in weak gel systems.

Flaxseed and hempseed flours were selected as model plant protein sources due to their increasing availability as oilseed processing side-streams and their contrasting compositional profiles, characterized by polysaccharide-rich versus protein-dominated network-forming components, respectively (Julakanti et al., 2023). This compositional diversity enables the investigation of distinct protein-polysaccharide interaction mechanisms and their impact on bulk and interfacial structuring behavior. Hydrocolloids such as carboxymethylcellulose and gum-based polymers are widely used to tailor viscosity, yield stress, and structural stability in concentrated dispersions (da Silva et al., 2018; Michaelis et al., 2023). Their interactions with plant proteins can influence hydration dynamics, entanglement density, and microstructural organization, ultimately affecting macroscopic deformation and flow behavior (Gao et al., 2024). Despite extensive studies on individual components, comparative investigations integrating different protein sources and hydrocolloid structuring strategies within a unified experimental framework remain limited.

Traditionally, the characterization of soft-solid systems has relied heavily on steady shear viscosity measurements. However, viscosity

* Corresponding author.
E-mail address: laura.piazza@unimi.it (L. Piazza).

https://doi.org/10.1016/j.lwt.2026.119443
Received 2 March 2026; Received in revised form 29 April 2026; Accepted 29 April 2026
Available online 1 May 2026

alone does not adequately capture the complex mechanical behavior of weak gels, which exhibit yield stress, shear-thinning, thixotropic recovery, and non-linear deformation under applied stress (Douglas, 2018). Moreover, the performance of structured soft-solids is influenced not only by bulk rheology but also by interfacial phenomena, including lubrication under confinement and adhesion to biological substrates. Soft tribology has emerged as a valuable approach to investigate lubrication regimes in structured materials under conditions of mixed and boundary friction (Sarkar et al., 2021). Complementary, mucoadhesion measurements provide insight into interfacial retention and adhesive interactions with biological tissues (Cook et al., 2017). While these techniques are increasingly applied independently, integrated multi-scale studies combining rheology, tribology, mechanical deformation, and ex-vivo mucoadhesion within plant protein-hydrocolloid systems remain scarce.

The present work aims to establish a multiscale characterization framework for flaxseed and hempseed protein-based soft-solid foods structured with different hydrocolloids and enzymatic treatments. By integrating rheological modeling, tribological analysis, back extrusion testing, and ex-vivo mucoadhesion measurements, this work elucidates how formulation variables modulate bulk mechanical response and interfacial performance across structured plant protein systems. In applied dysphagia context, soft-solid products are often described using texture-based classification systems. The International Dysphagia Diet Standardisation Initiative (IDDSI) provides a global framework for classifying texture-modified foods and liquids based on consistency (Cichero et al., 2017). In this study, IDDSI framework is used solely as a descriptive reference to contextualize instrumental rheological measurements. The work does not address clinical diagnostics or patient evaluation; all analyses and conclusions are based exclusively on physicochemical material characterization.

2. Materials and methods

2.1. Materials

Zucchini and salt were purchased from a local supermarket (Esselunga, Pioltello, Italy). Hempseed and flaxseed meals were obtained from a local market. Carboxymethylcellulose (CMC; molecular weight: 250,000 g/mol) was purchased from Sigma-Aldrich (Steinheim, Germany). High-acyl gellan gum (GHA) was purchased from CP Kelco (Atlanta, USA). The enzymes Viscozyme® (VISC) and Pectinase® (PECT) were purchased from Sigma-Aldrich. All the chemical reagents used for the analysis were purchased from Sigma-Aldrich. Fresh porcine oropharyngeal and esophageal tissues used in the mucoadhesion test were obtained from a local swine slaughterhouse (Lodi, Italy).

2.2. Chemical and physico-chemical characterization

Proteins in flours were concentrated by sieving to obtain controlled protein-rich fractions for structuring. A vibrating sieve shaker (Octagon 200, Endecotts Ltd, London, UK) equipped with 125 and 250 μm mesh sieves was used. Protein content after sieving was determined using the Kjeldahl method according to the AOAC (2023) procedure. The percentage of nitrogen was calculated according to Eq. (1), and the total protein content (g/100 g) was measured using 6.25 as the nitrogen conversion factor:

$$N = \frac{N(HCl)\cdot ml(HCl)\cdot 14}{Sample\ weight(g)\cdot 10} \quad (1)$$

The lipid component quantification of the 125 μm flours was performed by Soxhlet methodology following the AOAC (2023) procedure. Fat content (g/100 g) was calculated using Eq. (2):

$$Lipid = \frac{We}{Wt}\cdot 100 \quad (2)$$

where W_e is the weight of the extracted lipid content (g) and W_t is the total weight of the initial sample (g).

The dry matter (DM) of the 125 μm flours was determined following the AOAC (2023) procedure by weighing the material before and after drying in an oven (Gallenkamp Sanyo, Cambridge, UK). Results (g/100 g) were expressed using Eq. (3):

$$DM = \frac{Wa}{Ww}\cdot 100 \quad (3)$$

where W_w is the weight of the wet sample and W_a is the weight after drying.

Water holding capacity (WHC) and fat absorption capacity (FAC) were assessed according to the methods described by Hadnađev et al. (2018), with slight modifications. For WHC and FAC determination, 1.0 g of 125 μm flour was placed in a centrifuge tube, and 10.0 g of water, or 10.0 g of oil, was added for WHC and FAC measurements, respectively. The samples were stirred continuously for 30 min in order to promote absorption. Afterward, the samples were centrifuged (LISA MultiLab Centrifuge, AFI sarl, Château-Gontier, France) at 3000×g for 20 min. The supernatant was removed and the samples were carefully drained and weighed. Each determination was performed in triplicate, and the water holding capacity and oil absorption capacity were calculated according to Eq. (4):

$$WHC\ (or\ FAC) = \frac{Wh - Wd}{Wd}\cdot 100 \quad (4)$$

where W_d is the weight of the dry sample, while W_h is the weight of the sample after water, or oil, absorption.

2.3. Purees formulation

For each characterizing ingredient (flaxseed and hempseed flours), five formulations were prepared: a control (PLAIN) and four viscosity-modulated variants containing either hydrocolloids (CMC, GHA) or enzymes (VISC, PECT). The PLAIN formulation, containing no added hydrocolloids or enzymes, served as the reference matrix for evaluating the effect of each formulation strategy. All purees were processed using a Thermomix TM5 (Vorwerk, Wuppertal, Germany) to ensure a consistent thermal and shear history across formulations.

Preliminary trials (not reported) enabled the definition of a starting formulation meeting two target criteria: (i) protein providing 20% of total energy, thus fulfilling the requirements for the nutritional claim "high in protein" according to Regulation (EC) No. 1924/2006, and (ii) sodium content consistent with WHO recommendations for daily salt intake (≤ 5.0 g NaCl/day for a 2000 kcal diet), as outlined in the WHO Global Report on Sodium Intake Reduction (WHO, 2023).

The preparation protocol was as follows. Fresh zucchini were weighed and blended with the gradual addition of water (50% w/w of zucchini) until a homogeneous puree was obtained. Salt and either flaxseed or hempseed flour were then incorporated, and the mixture was cooked for 30 min at 80 °C with the lid on. This procedure yielded two PLAIN base formulations (zucchini, water, salt, and either flaxseed or hempseed flour). The subsequent addition of thickeners or enzymes, used at low levels, did not affect the total energy or macronutrient profile of the purees.

Viscosity-modulated purees were then obtained by incorporating structuring agents into the cooked PLAIN bases. For CMC samples, the hydrocolloid was added and homogenized to ensure uniform dispersion. For GHA samples, GHA was added and homogenized, followed by reheating to 80 °C and subsequent cooling (Morris et al., 2012). The concentrations of thickeners were selected based on preliminary unpublished trials, in which a wider dosage range was screened to identify levels yielding homogeneous and stable purees with clearly distinguishable structuring effects. For VISC and PECT samples, the enzymes Viscozyme® and Pectinase®, respectively, were incorporated as described in previous work (Piazza et al., 2023).

To contextualize the prototype purees within real-use conditions, their consistency was assessed according to the IDDSI framework using the standardized Flow Test (10 mL syringe method). Samples were classified as Level 2 (Mildly thick), Level 3 (Moderately thick), or Level 4 (Extremely thick). Samples classified as Levels 3 and 4 were further evaluated using the IDDSI Fork Drip Test and Spoon Tilt Test (Cichero et al., 2017).

2.4. Rheological and viscoelasticity assessment

Rheological properties of the purees were obtained using a combined motor transducer rheometer (DHR-2, TA Instruments, New Castle, USA), equipped with a 40 mm diameter cone-plate geometry. During all tests temperature was kept constant at 25 ± 0.1 °C and a solvent trap was used to prevent loss of solvent. Shear flow tests were run in triplicate in the range 0.01-1000 s^{-1}. Data were modelled using Herschel-Bulkley Eq. (5) to evaluate shear-thinning behavior and to obtain the rheological parameters:

$$\sigma = \sigma_0 + k \cdot \dot{\gamma}^n \quad (5)$$

where σ is the shear stress (Pa), σ_0 is the yield stress (Pa), K is the consistency index (Pa·s^n), $\dot{\gamma}$ is the shear rate (s^{-1}) and n is the flow behavior index (dimensionless). The chosen shear rate range enabled to determine the oral-relevant viscosities according to (Bolivar-Prados et al., 2022; Ross et al., 2019).

Following, the viscosity recovery of the samples was recorded using the 3 Intervals Thixotropy Test (3ITT), applying the following shear rates: 0.1 s^{-1} in the first and third intervals (each lasting 60 s), and 100 s^{-1} in the second interval (lasting 120 s) (Cuomo et al., 2021). Tests were run in triplicate and the percentage recovery was calculated by comparing the final viscosity with the initial viscosity, according to Eq. (6):

$$Thixotropy = \frac{\eta_f}{\eta_0} \cdot 100 \quad (6)$$

where η_f is the viscosity (Pa·s) measured during the third interval and η_0 is the initial viscosity (Pa·s).

Viscoelastic properties of purees were evaluated through oscillatory measurements using a DHR-2 rheometer fitted with a 40 mm diameter parallel plate geometry and a gap distance of 1 mm, at a constant temperature of 25 ± 0.1 °C. The linear viscoelastic region (LVR) was determined using amplitude sweep tests by increasing strain amplitude from 0.01% to 100% at a fixed frequency of 1 Hz. Frequency sweep tests were subsequently performed within the established LVR (strain amplitude equal to 0.5%), covering a frequency range of 0.1-100 Hz. All measurements were conducted in triplicate. The elastic modulus (G′, Pa) and the viscous modulus (G’’, Pa), of the complex modulus (G*, Pa) were retrieved and analyzed.

2.5. Texture properties

Back extrusion tests were performed using a TA-XT2 texture analyzer (Stable MicroSystems Ltd, Godalming, UK) equipped with a 50 Kg load cell and a specific geometry (A/BE) consisting of a cylindrical acrylic cup and a 40-mm diameter Plexiglas disk probe. The cup was filled with the sample with a thickness of 20 mm and the following parameters were used: pre-test velocity 1 mm/s, test velocity 2 mm/s, post-test velocity 10 mm/s, force equal to 5 g (Ibañez et al., 2022). Under uniaxial loading, the product was extruded upward and around the edge of the disk when the samples were compressed to a depth of 10 mm. Mechanical data were recorded using Texture Exponent v3.2 (Stable MicroSystems Ltd), and the following parameters were evaluated: Maximum positive force (N), Positive area (N·mm), and Negative area (N·mm). Samples were analyzed in quadruplicate at room temperature, and results expressed as mean ± standard deviation.

2.6. Mucoadhesion assessment

The mucoadhesive capacity of purees under study was quantified using an ex-vivo compression-detachment test on porcine mucosae, which are employed as biologically representative substrates due to their structural similarity to human oral and esophageal tissues (Garcia-Tarazona et al., 2023). Mucoadhesion tests were conducted on three distinct porcine tissues – tongue, soft palate, and esophagus – selected to represent different morphological characteristics and consequently biological interfaces.

Mucoadhesion was evaluated using a TA-XT2 texture analyzer equipped with a 50 kg load cell and a specific mucoadhesion test rig (A/MUC). Fresh porcine mucosa was carefully excised, trimmed to remove underlying tissue, rinsed with physiological saline, gently blotted to remove excess surface moisture, and mounted onto the central holder of the A/MUC rig with the mucosal surface facing upward (Fig. 1).

A fixed sample volume (1.0 mL) was loaded onto the testing probe. The probe was lowered toward the mucosal surface at a constant speed of 0.5 mm/s until contact was established. A constant normal force of 0.5 N was then applied and maintained for 30 s to allow the formation of adhesive interactions between the sample and the mucosa (Pestana et al., 2024).

Subsequently, the probe was withdrawn at the same speed (0.5 mm/s) until complete detachment. The force-distance curve generated during the detachment phase was recorded using Texture Exponent software (v3.2). From these curves, two parameters were determined: (i) peak detachment force (Peak, N), defined as the maximum force required to initiate separation, and (ii) work of adhesion (W_{ADH}, N·mm), calculated as the area under the force-distance curve, representing the total energy required for detachment (Bassi da Silva et al., 2017). These parameters describe both the strength and the persistence of mucoadhesion (Thirawong et al., 2007).

All measurements were performed at room temperature in quintuplicate, using independently prepared mucosal samples and puree aliquots. Results are reported as mean ± standard deviation.

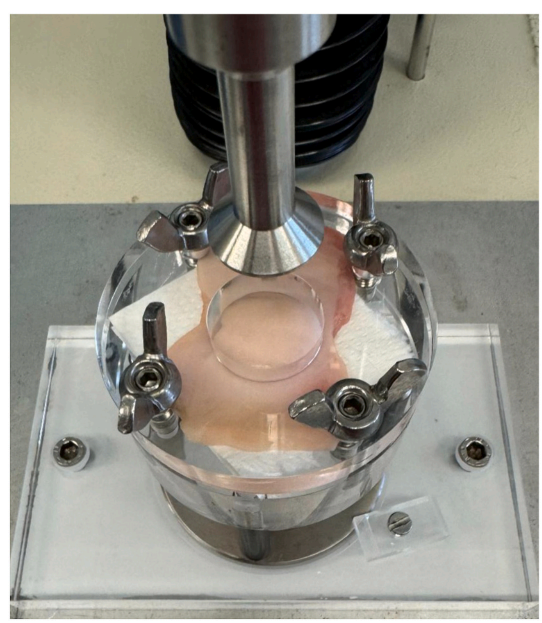

Fig. 1. TA-XT2 texture analyzer equipped with the A/MUC mucoadhesion rig. The selected porcine tissue (esophagus shown) was secured in the sample holder, while the puree was placed on the descending probe prior to controlled contact-detachment testing protocol.

2.7. Tribological analysis

Tribological measurements were performed in triplicate using a ball-on-three-plates geometry mounted on DHR-2 rheometer, at a constant temperature of 37 ± 0.1 °C. Sliding velocity was increased logarithmically from 10^{-6} to 10^{0} m/s, under a constant normal force (F_N) of 2.5 N (Principato et al., 2024). The normal load was zeroed prior to each measurement and automatically maintained throughout the test. During the test the coefficient of friction (μ, dimensionless), was determined according to Eq. (7):

$$\mu = \frac{M \cdot \cos\beta}{d \cdot \sin\beta \cdot F_N} = \frac{M}{d \cdot F_N} \tag{7}$$

where M is the torque (N·m), β is the angle between the probe and the plates (45°), F_N is the normal force (N) and d is the arm length (m). The results were obtained as variation of the friction coefficient as a function of the sliding speed, in the form of Stribeck curve.

2.8. Statistical analysis

Data were analyzed using RStudio (v2026.01.0+392; R Core Team, R Foundation for Statistical Computing, Vienna, Austria). Independent-samples t-tests were used to compare the proximate composition of flaxseed and hempseed flours ($p < 0.05$). A two-way analysis of variance (ANOVA) was performed to assess the effects of flour matrix type (flax vs hemp), hydrocolloid type and their interaction on the purees' textural and mucoadhesive parameters. Tukey-Kramer's HSD post hoc test was used for multiple comparisons, and differences were considered statistically significant at $p < 0.05$.

3. Results and discussion

The oral processing of structured soft-solids is not fully captured by flow behavior alone. In these systems, performance arises from the interplay between bulk mechanical properties and interfacial interactions under low deformation and confined conditions.

Weak gel systems, such as vegetable-based purees, require limited mastication; however, their in-mouth behavior is strongly influenced by resistance to deformation, structural recovery, lubrication properties, and interactions with oral surfaces (Nishinari et al., 2020). Therefore, a comprehensive description requires the integration of rheological, mechanical, and tribological descriptors, rather than relying solely on viscosity.

In this study, zucchini-based plant protein formulations structured with hydrocolloids or enzymatically modified were used as model soft-solid systems to explore these contributions. From a physicochemical perspective, particular attention was given to the role of protein source and structuring strategy in modulating both network formation and interfacial behavior. By generating formulations spanning a range of consistencies, the experimental design enabled a systematic comparison of yield stress, deformation resistance, lubrication regimes, and mucoadhesive interactions within a unified multiscale framework.

Although no formal sensory evaluation was conducted, instrumental parameters such as yield stress, extrusion force, and friction coefficient are widely recognized as relevant indicators of perceived thickness, cohesiveness, and smoothness in structured food systems (Chen et al., 2026; Dhamodharan et al., 2025). In this context, the present approach provides a more comprehensive interpretation of oral processing than viscosity-based descriptions alone.

The protein-rich flour ingredients used in the formulations were mildly pretreated by sieving through different mesh sizes (data not shown) to remove most of the fiber, resulting in increased protein content. For both flaxseed and hempseed flours, the 125 μm fraction showed the highest protein content. As reported in Table 1, the comparative analysis of the sieved flaxseed and hempseed flours also revealed differences in functional attributes beyond compositional aspects.

Table 1
Compositional characterization of flaxseed and hempseed flours (125 μm). All values are expressed in g/100 g.

	Flaxseed flour	Hempseed flour
Protein	33.7 ± 0.2 [a]	26.4 ± 0.6 [b]
Lipid	9.5 ± 0.1 [a]	9.1 ± 0.1 [a]
DM	92.2 ± 0.3 [a]	92.8 ± 0.4 [a]
WHC	0.63 ± 0.1 [a]	0.17 ± 0.1 [b]
FAC	0.15 ± 0.1 [a]	0.13 ± 0.1 [a]

Within each row, different letters (a, b) indicate significant differences between samples ($p < 0.05$). DM: dry matter; WHC: water holding capacity; FAC: fat absorption capacity.

Flaxseed flour exhibited a higher water-holding capacity, a property that may influence texture and stability in semi-solid matrices such as purees, while fat absorption capacity was similar for both flours. Purees were formulated to ensure that at least 20% of the total caloric content derived from proteins, enabling the use of the "high in protein" nutritional claim (Reg. 1924/06/EC). Consequently, the amount of flour incorporated in each formulation was calculated based on its protein contribution relative to the total energy content of the puree.

Due to the different intrinsic protein contents of flaxseed and hempseed flours (Table 1), this approach required slight adjustments in the relative proportions of ingredients, resulting in modest differences in the zucchini and water content between flax- and hemp-based formulations (Table 2). These variations reflect the constraint of maintaining equivalent nutritional targets across systems, rather than an intentional modification of the solid fraction. A formulation at equal solid content would not have ensured nutritional equivalence and would therefore be less representative of realistic product design.

Salt concentration was controlled according to WHO (2023) recommendations (≤ 5.0 g NaCl/day for a 2000 kcal diet). Accordingly, the salt content of each puree (< 0.1 wt%) was calculated based on total caloric value, ensuring compliance with dietary sodium limits while maintaining palatability.

For each of the two base formulations (flax PLAIN or hemp PLAIN), viscosity-modulating agents were incorporated to achieve consistencies suitable for oral-processing studies. Among the hydrocolloids tested, CMC (1.0 wt%) and GHA (0.2 wt%) were effective thickeners, with GHA showing functionality even at low concentration (Huang et al., 2008). Enzyme blends were also included for their pectinolytic (PECT) and cellulolytic (VISC) activities, applied under optimized conditions (3.0 μL/g) established in previous work (Piazza et al., 2023).

Each flax- and hemp-based preparation was used to generate five samples, resulting in the ten formulations reported in Table 2. It should be noted that the compositional differences between flax- and hemp-based systems may contribute to variations in rheological parameters; however, these effects are intrinsically linked to the formulation strategy adopted and should be interpreted in conjunction with the overall structural and functional behavior of the systems.

3.1. Flow properties of plant protein-hydrocolloid soft-solids

Viscosity is a key descriptor of deformation and flow behavior in structured soft-solids, as it governs resistance to shear under oral-like conditions. Flow curves were obtained for each prototype formulation and are shown in Fig. 2.

All samples exhibited pronounced shear-thinning behavior, characteristic of weakly structured semi-solid systems. The Herschel-Bulkley model was applied (Eq. (5)) and the fitted rheological parameters are reported in Table 3.

The model confirmed $n < 1$ for all samples, indicating non-Newtonian flow behavior, with apparent viscosity decreasing as shear rate increased. Both hydrocolloid type and protein source significantly affected the rheological response. The addition of CMC and GHA

Table 2
Formulation of plant-based monophase purees.

	Sample	Zucchini (% wt)	Water (% wt)	Flaxs (% wt)	Hemps (% wt)	CMC	GHA	VISC	PECT	Salt
Flax based	**PLAIN**	64.00	32.08	3.85	-	-	-	-	-	+
	CMC	64.00	32.08	3.85	-	+	-	-	-	+
	GHA	64.00	32.08	3.85	-	-	+	-	-	+
	VISC	64.00	32.08	3.85	-	-	-	+	-	+
	PECT	64.00	32.08	3.85	-	-	-	-	+	+
Hemp based	**PLAIN**	68.30	27.73	-	3.90	-	-	-	-	+
	CMC	68.30	27.73	-	3.90	+	-	-	-	+
	GHA	68.30	27.73	-	3.90	-	+	-	-	+
	VISC	68.30	27.73	-	3.90	-	-	+	-	+
	PECT	68.30	27.73	-	3.90	-	-	-	+	+

Flaxs: flaxseed flour (125 μm); Hemps: hempseed flour (125 μm); CMC: carboxymethylcellulose; GHA: high-acyl gellan gum; VISC: viscozyme; PECT: pectinase.

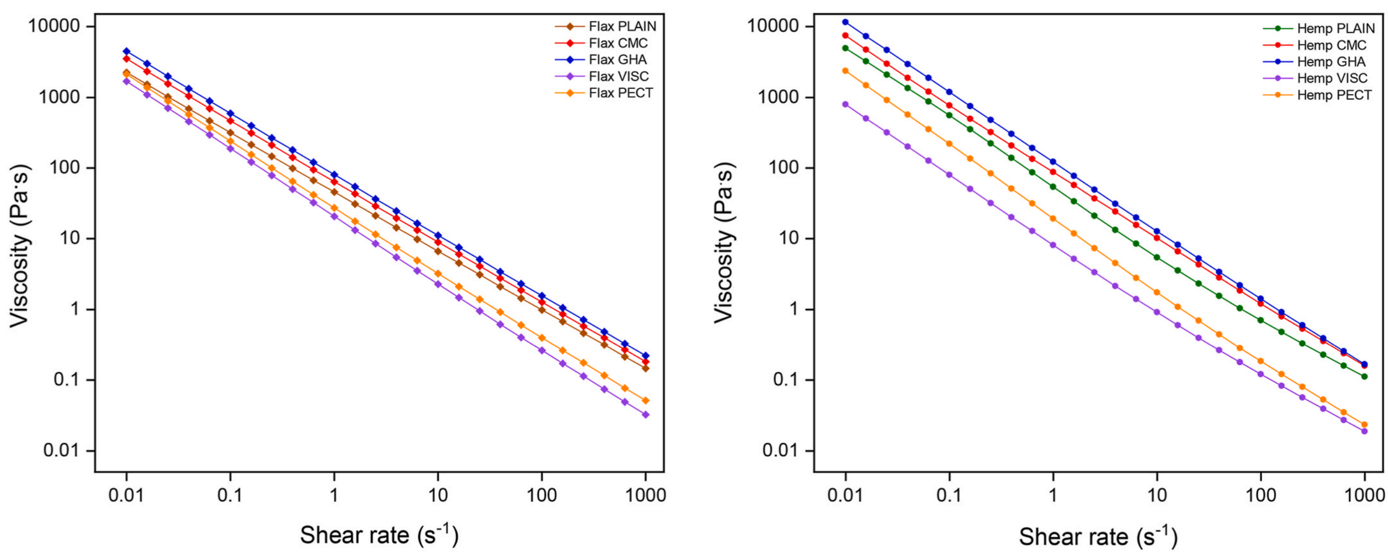

Fig. 2. Flow curves of flaxseed-based (left) and hempseed-based (right) purees.

Table 3
Rheological parameter obtained from the Herschel-Bulkley model.

	Flax-based					Hemp-based				
	PLAIN	CMC	GHA	VISC	PECT	PLAIN	CMC	GHA	VISC	PECT
σ_0 (Pa)	4.58	11.04	11.71	1.69	1.44	5.90	12.91	17.75	4.33	4.53
K (Pa·s^n)	41.45	53.22	69.37	18.63	17.41	45.53	53.59	70.58	27.61	26.77
n (–)	0.18	0.17	0.16	0.19	0.19	0.18	0.16	0.16	0.19	0.22
R^2	0.99	0.99	0.99	0.99	0.99	0.99	0.99	0.99	0.99	0.99

σ0: yield stress; K: consistency index; n: flow behavior index. CMC: carboxymethylcellulose; GHA: high-acyl gellan gum; VISC: viscozyme; PECT: pectinase.

increased yield stress (σ_0) and consistency index (K) in both flax- and hemp-based matrices, reflecting enhanced structural cohesion and network reinforcement. Among the structuring strategies, GHA produced the highest σ_0 and K values and the lowest flow behavior index (n), consistent with the development of a weak gel-like structure. In contrast, enzymatic treatments (VISC and PECT samples) markedly reduced σ_0 and K and increased n, indicating network disruption and a shift toward more fluid-like behavior due to polysaccharide and pectin hydrolysis.

When comparing protein sources, hemp-based systems generally exhibited higher σ_0 and K values than their flax-based counterparts formulated with the same structuring components, although they also had higher total solids content. This suggests that hemp protein contributes to a denser and more interconnected matrix, potentially owing to its higher insoluble fraction and stronger particle-hydrocolloid interactions. Flax-based systems showed comparatively lower yield stress and viscosity, possibly due to differences in protein solubility and endogenous mucilage content (Lorenc et al., 2022), which may interfere with hydrocolloid-driven network formation.

To contextualize deformation behavior under oral-like shear conditions, apparent viscosities were extrapolated at 10, 50, and 300 s^{-1}, which are commonly used as reference shear rates in texture-modified food research (Bolivar-Prados et al., 2022; Cichero et al., 2017; Ross et al., 2019). These values are presented in Table 4 together with the corresponding IDDSI consistency levels, used here as a practical reference.

At 10 s^{-1}, substantial formulation-dependent differences were

Table 4
Apparent viscosity (η) calculated at 10, 50, and 300 s^{-1} for formulated purees and retrieved IDDSI classification.

		η Flax-based (Pa·s)					η Hemp-based (Pa·s)				
		PLAIN	CMC	GHA	VISC	PECT	PLAIN	CMC	GHA	VISC	PECT
$\dot{\gamma}$ (s^{-1})	**10**	6.75 ±0.10	9.01 ±0.11	11.24 ±0.14	3.06 ±0.08	2.84 ±0.07	7.50 ±0.09	9.04 ±0.04	11.94 ±0.11	4.71 ±0.10	4.90 ±0.07
	50	1.78 ±0.02	2.31 ±0.03	2.85 ±0.04	0.82 ±0.03	0.74 ±0.02	1.97 ±0.02	2.26 ±0.03	2.95 ±0.02	1.25 ±0.03	1.36 ±0.02
	300	0.40 ±0.01	0.51 ±0.02	0.62 ±0.01	0.19 ±0.02	0.18 ±0.01	0.45 ±0.01	0.49 ±0.01	0.65 ±0.02	0.29 ±0.01	0.33 ±0.02
	IDDSI level	3	4	4	2	2	3	4	4	2	2

CMC: carboxymethylcellulose; GHA: high-acyl gellan gum; VISC: viscozyme; PECT: pectinase.

observed. GHA and CMC increased low-shear viscosity, indicating higher resistance to initial deformation, whereas enzyme-treated systems exhibited markedly lower viscosities, consistent with reduced structural integrity.

At 50 s^{-1}, viscosity values reflected the flow behavior typically associated with oral processing and swallowing conditions, providing an empirical reference point for comparing consistency across samples. PLAIN flax- and hemp-based systems fell within intermediate viscosity ranges, while hydrocolloid-enriched samples shifted toward higher consistency classes. Enzyme-treated samples (VISC and PECT) corresponded to lower viscosity categories, reflecting their more fluid-like character.

At 300 s^{-1}, all samples showed pronounced viscosity reduction, confirming strong shear-thinning behavior and the ability of the network to undergo rapid structural breakdown under high deformation rates. Notably, GHA-structured systems combined elevated low-shear viscosity with substantial viscosity reduction at high shear, indicating a favorable balance between structural stability at rest and deformability under flow.

Overall, the results demonstrate that hydrocolloid structuring and enzymatic modulation provide effective tools for tuning yield stress and shear-dependent viscosity within empirically defined consistency classes, while maintaining distinct network architectures governed by protein source and polymer interactions.

3.2. *Thixotropic behavior and structural recovery under shear*

The time-dependent response of structured soft-solids to shear deformation provides insight into network resilience and the material's ability to recover its internal structure after disruption. Under dynamic oral-like conditions, materials undergo sequential phases of low deformation, high shear, and subsequent relaxation. Characterizing thixotropic behavior is therefore essential to understanding how structural breakdown and recovery contribute to overall texture performance.

Thixotropy was evaluated using a three-interval thixotropy test (3ITT), in which samples were subjected sequentially to a low-shear phase (rest), a high-shear phase (structural breakdown), and a final low-shear phase (recovery). This protocol allows quantification of both viscosity loss under high shear and the extent of structural rebuilding once shear is reduced (Piazza et al., 2023).

Across all formulations high recovery values were observed, indicating substantial structural resilience. Plain purees exhibited an average recovery of 87%, reflecting a robust intrinsic network. The incorporation of hydrocolloids further enhanced recovery, with values ranging from 90% to 94%. Among all systems, GHA-structured purees showed the highest recovery (94%), demonstrating a pronounced ability to re-establish network integrity after shear-induced disruption. This behavior is consistent with weak gel formation and reversible polymer-polymer interactions that facilitate rapid structural rebuilding. Enzymatically treated systems, although characterized by lower viscosity and yield stress, maintained relatively high recovery values, suggesting that even partially disrupted networks retain sufficient structural connectivity to be rebuilt under low shear conditions.

Quantifying thixotropic breakdown and recovery provides information complementary to that obtained from steady-shear viscosity. Whereas viscosity defines resistance to flow at specific shear rates, thixotropy describes the kinetics of structural breakdown and rebuilding. Taken together, these parameters allow a more comprehensive assessment of how formulation variables modulate deformation resistance, structural stability, and post-shear recovery capacity.

Overall, the results indicate that hydrocolloid type predominantly governs recovery efficiency, whereas protein source influences baseline structural strength. The integration of steady and time-dependent rheological measurements therefore strengthens the structure-function interpretation of plant protein-hydrocolloid soft-solids under dynamic deformation conditions.

3.3. *Ex-vivo mucoadhesion and interfacial retention behavior*

Mucoadhesion refers to the ability of a structured soft-solid to establish adhesive interactions with biological mucosal surfaces. In the context of oral processing, these interfacial interactions play a key role in governing retention, detachment, and bolus transport under confined conditions. Hydrocolloids and proteins can exhibit markedly different affinities for mucosal substrates, depending on their molecular structure and interaction mechanisms (Cook et al., 2017).

In this study, ex-vivo mucoadhesion measurements were performed to characterize formulation-dependent interfacial behavior across samples with different consistency levels. Results are presented in Tables 5 and 6, with representative force-time curves shown in Fig. 3.

The measured adhesion can be understood as the result of two coupled contributions: interfacial physiochemistry – including with hydrogen bonding, electrostatic and dispersive interactions between polymer/protein domains and tissue components (Bayer, 2022) – and mechanical interlocking driven by tissue roughness and surface features, which is particularly relevant in the oral cavity (Cook et al., 2017). Plant-derived proteins and hydrocolloids offer different combinations of surface charge, hydration layer structure, and chain mobility, which influence tissue wetting, formation of effective contact area, and the size and strength of adhesive fibrils that develop during separation. In this context, Peak and W_{ADH} serve as macroscopic descriptors of how each protein-hydrocolloid network mechanically couples to the underlying tissue topography.

Mucoadhesion tests were conducted on three distinct porcine oropharyngeal and esophageal tissues. The anatomical and compositional differences among these tissues (papillated versus relatively smooth epithelia, and varying surface roughness) enabled assessment of how each formulation interacts with biologically heterogeneous interfaces.

On tongue mucosa, flaxseed-based formulations exhibited higher detachment force and W_{ADH} than hemp-based counterparts, indicating stronger interfacial interactions and greater short-term retention on this rough, papillated surface. Hemp-based systems showed lower adhesion values, reflecting weaker surface affinity and more readily reversible contact.

Table 5
Mucoadhesion test results on porcine tongue mucosa.

	Flax-based					Hemp-based				
	PLAIN	CMC	GHA	VISC	PECT	PLAIN	CMC	GHA	VISC	PECT
W_{ADH} (N·mm)	0.56 ± 0.07 ^{c}	0.59 ± 0.10 ^{b}	0.69 ± 0.04 ^{a}	0.46 ± 0.05 ^{e}	0.50 ± 0.04 ^{e}	0.30 ± 0.03 ^{e}	0.35 ± 0.05 ^{e}	0.50 ± 0.16 ^{d}	0.13 ± 0.05 ^{f}	0.13 ± 0.07 ^{f}
Peak (N)	0.39 ± 0.04 $^{a;b}$	0.40 ± 0.04 $^{a;b}$	0.41 ± 0.02 ^{a}	0.34 ± 0.03 $^{b;c}$	0.37 ± 0.02 ^{b}	0.26 ± 0.01 ^{d}	0.30 ± 0.03 $^{c;d}$	0.38 ± 0.07 ^{b}	0.13 ± 0.02 ^{e}	0.13 ± 0.07 ^{e}

Within each row, different letters (a-f) indicate significant differences between formulations ($p < 0.05$). Peak: peak detachment force; WADH: work of adhesion. CMC: carboxymethylcellulose; GHA: high-acyl gellan gum; VISC: viscozyme; PECT: pectinase.

Table 6
Mucoadhesion test results on porcine soft palate mucosa.

	Flax-based					Hemp-based				
	PLAIN	CMC	GHA	VISC	PECT	PLAIN	CMC	GHA	VISC	PECT
W_{ADH} (N·mm)	0.73 ± 0.05 ^{b}	0.82 ± 0.13 ^{a}	0.88 ± 0.11 ^{a}	0.51 ± 0.07 ^{c}	0.52 ± 0.09 ^{c}	0.42 ± 0.12 ^{d}	0.56 ± 0.14 ^{c}	0.86 ± 0.20 ^{a}	0.14 ± 0.05 ^{e}	0.15 ± 0.02 ^{e}
Peak (N)	0.35 ± 0.01 $^{b;c}$	0.48 ± 0.05 ^{a}	0.48 ± 0.02 ^{a}	0.27 ± 0.13 ^{d}	0.27 ± 0.02 ^{d}	0.32 ± 0.07 ^{c}	0.39 ± 0.07 $^{b;c}$	0.51 ± 0.05 ^{a}	0.17 ± 0.02 ^{e}	0.17 ± 0.02 ^{e}

Within each row, different letters (a-e) indicate significant differences between formulations ($p < 0.05$). Peak: peak detachment force; WADH: work of adhesion. CMC: carboxymethylcellulose; GHA: high-acyl gellan gum; VISC: viscozyme; PECT: pectinase.

Table 7
Mucoadhesion test results on porcine esophageal mucosa.

	Flax-based					Hemp-based				
	PLAIN	CMC	GHA	VISC	PECT	PLAIN	CMC	GHA	VISC	PECT
W_{ADH} (N·mm)	0.41 ± 0.14 ^{b}	0.50 ± 0.07 ^{a}	0.53 ± 0.12 ^{a}	0.23 ± 0.07 ^{d}	0.21 ± 0.02 ^{d}	0.11 ± 0.06 ^{e}	0.17 ± 0.05 ^{c}	0.23 ± 0.10 $^{b;c}$	0.11 ± 0.04 ^{e}	0.08 ± 0.05 ^{e}
Peak (N)	0.20 ± 0.08 $^{a;b}$	0.22 ± 0.04 ^{a}	0.24 ± 0.05 ^{a}	0.11 ± 0.03 ^{c}	0.10 ± 0.01 ^{c}	0.08 ± 0.01 ^{c}	0.09 ± 0.01 ^{c}	0.16 ± 0.05 ^{b}	0.04 ± 0.01 ^{d}	0.03 ± 0.02 ^{d}

Within each row, different letters (a-e) indicate significant differences between formulations ($p < 0.05$). Peak: peak detachment force; WADH: work of adhesion. CMC: carboxymethylcellulose; GHA: high-acyl gellan gum; VISC: viscozyme; PECT: pectinase.

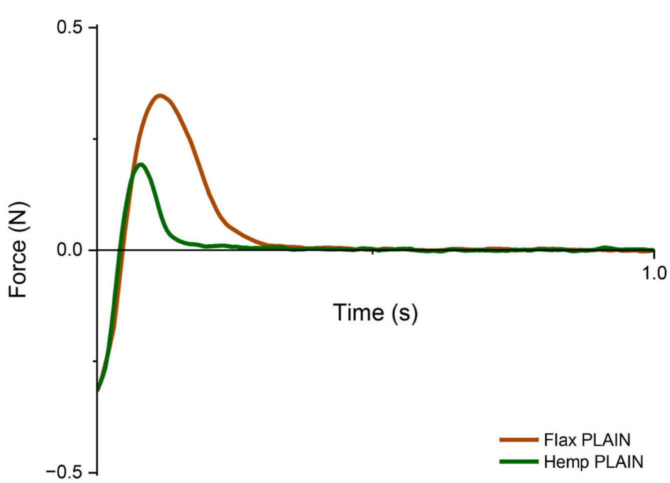

Fig. 3. Representative mucoadhesion profile (Force vs Time) obtained for flaxseed-based (brown) and hempseed-based (green) PLAIN purees on fresh porcine tongue mucosa.

On soft palate mucosa, mucoadhesion values increased across all samples, suggesting enhanced surface engagement on this substrate compared to tongue tissue. The trend remained consistent, with flax-based formulations displaying higher adhesion than hemp-based ones. The overall increase in both mucoadhesion parameters can be mechanistically attributed to the greater deformability of the soft palate, which likely promotes enhanced spreading and conformational adaptation of the bolus to the tissue surface under compression, thereby increasing the effective contact area and the number of load-bearing adhesive junctions.

On esophageal mucosa, a general reduction in both detachment force and W_{ADH} was observed for all formulations, consistent with the smoother morphology and lower apparent roughness reported for esophageal tissue (de Araújo et al., 2021).

The adhesion behavior across tissues reflects a gradient of interfacial interactions governed by mucosal structure and mechanics, indicating that retention depends on both physicochemical properties and substrate morphology. Accordingly, oral behavior is substrate-specific rather than purely intrinsic.

Across all tissues, hydrocolloid addition significantly modulated adhesive behavior. GHA consistently produced the highest detachment forces and adhesion energies in both flax- and hemp-based systems, confirming its dual role as a structuring agent and surface-interactive polymer. GHA likely forms hydrated, compliant networks that adapt to tissue micro-topography and sustain fibrillation during debonding, potentially contributing to increased Peak and W_{ADH} (Carvalho et al., 2010). CMC also enhanced adhesion relative to PLAIN samples, though to a lesser extent. This is in line with previous studies suggesting that anionic cellulose derivatives may enhance bioadhesion via hydrogen bonding and favorable wetting, while their semi-flexible chains may contribute to stable filament formation during tensile separation (Carvalho et al., 2010).

In contrast, enzymatic treatments (VISC and PECT) substantially reduced adhesive strength, likely due to partial disruption of polymer-mucosa interactions and reduced surface-binding capacity following structural hydrolysis.

These results indicate that interfacial retention is influenced by both protein source and hydrocolloid architecture, reflecting differences in structural cohesion and surface interactions that are not captured by bulk flow properties alone.

Although standardized benchmarks for mucoadhesive performance in texture-modified food systems are currently lacking, the present data provide quantitative reference values and identify flaxseed protein and high-acyl gellan gum as promising structuring components for enhancing interfacial retention while preserving deformability. The definition of material-based reference ranges for mucoadhesion may support more comprehensive structure-function characterization of soft-solid food matrices.

3.4. Back extrusion analysis and macrostructural texture under compression

Building on rheological, thixotropic, and mucoadhesive characterization, back extrusion testing was performed to evaluate the macrostructural mechanical response of the formulated soft-solids under compressive and extensional deformation. While mucoadhesion elucidates interfacial interactions with biological substrates, back extrusion testing provides a bulk mechanical assessment of resistance to deformation and structural integrity under confined compression.

This method quantifies parameters such as maximum extrusion force, positive work of deformation (mechanical cohesiveness), and negative area during probe withdrawal (adhesive work), which are closely related to firmness, internal stability, and structural continuity (Ascrizzi & Piazza, 2025; Baixauli et al., 2022). Back extrusion analysis has been widely adopted for characterizing soft-solid systems subjected to compressive stress conditions representative of tongue-palate deformation (Ibañez et al., 2022). As such, it offers a complementary mechanical perspective linking microstructural modifications to macroscopic consistency differences (Lee et al., 2025). Results are shown in Table 8.

Flaxseed-based formulations exhibited higher extrusion forces and positive work values than their hemp-based counterparts, indicating greater resistance to deformation and stronger internal cohesion. These findings are consistent with the higher yield stress values observed in shear rheology and support the presence of a more connected structural network in flax-based systems.

In contrast, hemp-based formulations showed lower extrusion forces and reduced mechanical cohesiveness, reflecting a less continuous matrix under compression. At the mesoscale, these differences may be related to compositional factors: flaxseed protein concentrates contain higher levels of soluble fiber and exhibit greater water-holding capacity, which can promote the formation of a more cohesive matrix (Kučka et al., 2024), whereas the higher insoluble fraction in hemp-based systems may disrupt matrix continuity and reduce resistance under compressive load (Karabulut et al., 2023).

Hydrocolloid type and enzymatic treatment further modulated textural behavior. GHA significantly increased extrusion force, deformation work, and adhesive work, confirming its strong network-forming and reinforcement capacity. CMC also enhanced structural parameters, although to a lesser extent. Conversely, enzymatic treatments reduced extrusion forces and deformation work, reflecting matrix softening and increased deformability associated with partial structural breakdown.

A clear correspondence was observed between yield stress (σ_0) derived from flow curve analysis and extrusion force measured by back extrusion. Formulations with higher σ_0 exhibited greater resistance to compressive deformation, with GHA-enriched systems showing the highest values and enzyme-treated samples the lowest. This consistency suggests that stronger internal networks require greater force to initiate deformation under both shear and compression (Perrot et al., 2011). Accordingly, samples with higher yield stress also displayed increased positive work of deformation, indicating enhanced cohesiveness and matrix integrity.

Overall, back extrusion results highlight the influence of formulation variables on compressive resistance and structural cohesion in plant protein-hydrocolloid soft-solids.

3.5. Purees' rheology at the mesoscale

Dynamic rheological measurements further supported the structural interpretation derived from steady-shear and mechanical analyses. Frequency sweep tests revealed a characteristic weak gel-like behavior in all formulations, with the storage modulus (G') consistently higher than the loss modulus (G'') over the entire frequency range (Fig. 4). This viscoelastic profile represents a favorable structural configuration for soft-solid foods intended for controlled oral processing: weak gels maintain structural integrity at rest while yielding under applied stress, thereby allowing cohesive deformation under oral shear conditions. Unlike strong gels that resist compression or fluid dispersions that lack internal cohesion, weak gels provide a balanced combination of elasticity and deformability (Giura et al., 2021).

Within this weak-gel framework, formulation-dependent differences were evident. Flaxseed-based purees displayed higher G' values and lower frequency dependence than hempseed-based systems, indicating stronger and more interconnected network architectures. This behavior can be attributed to the polysaccharide-rich composition of flaxseed – particularly arabinoxylans, glucans, and rhamnogalacturonan I – which form three-dimensional networks through chain entanglement, hydrogen bonding, and ionic interactions (Troshchynska et al., 2022). These structures promote stress distribution and elastic recovery, resulting in cohesive and mechanically resilient matrices (Alfaro-Rodríguez et al., 2024). In contrast, hempseed-based formulations rely predominantly on protein-protein interactions (e.g., disulfide bonding and hydrophobic aggregation), leading to less interconnected and more frequency-dependent networks (Mendoza-Pérez et al., 2024). This structural organization is consistent with the lower extrusion forces and reduced mucoadhesive responses previously observed, confirming the comparatively limited crosslinking density of protein-dominated systems.

The incorporation of hydrocolloids significantly modulated viscoelastic behavior. GHA markedly increased G', indicating partial gel reinforcement and the development of continuous polysaccharide-protein networks. This structural strengthening, coherently reflected

Table 8
Back extrusion test parameters of formulated purees.

	Flax-based					Hemp-based				
	PLAIN	CMC	GHA	VISC	PECT	PLAIN	CMC	GHA	VISC	PECT
Positive peak (N)	1.73 ± 0.08 [b]	0.78 ± 0.01 [c;d]	2.10 ± 0.16 [a]	0.51 ± 0.02 [e;f]	0.66 ± 0.01 [d;e]	0.86 ± 0.03 [c]	0.39 ± 0.01 [f;g]	1.84 ± 0.07 [b]	0.20 ± 0.01 [h]	0.26 ± 0.01 [g;h]
Positive area (N·mm)	11.6 ± 0.68 [b]	6.23 ± 0.10 [c]	13.59 ± 1.64 [a]	4.24 ± 0.17 [d;e]	5.39 ± 0.08 [d]	6.63 ± 0.34 [c;d]	3.28 ± 0.01 [e]	12.85 ± 1.11 [a;b]	1.86 ± 0.06 [f]	2.62 ± 0.09 [f]
Negative area (N·mm)	9.66 ± 0.81 [b]	7.59 ± 0.07 [c]	11.52 ± 0.48 [a]	2.14 ± 0.12 [f]	2.89 ± 0.22 [e;f]	3.23 ± 0.21 [e]	2.52 ± 0.04 [e;f]	6.33 ± 0.83 [d]	0.47 ± 0.08 [g]	0.73 ± 0.03 [g]

Within each row, different letters (a-h) indicate significant differences between formulations ($p < 0.05$). CMC: carboxymethylcellulose; GHA: high-acyl gellan gum; VISC: viscozyme; PECT: pectinase.

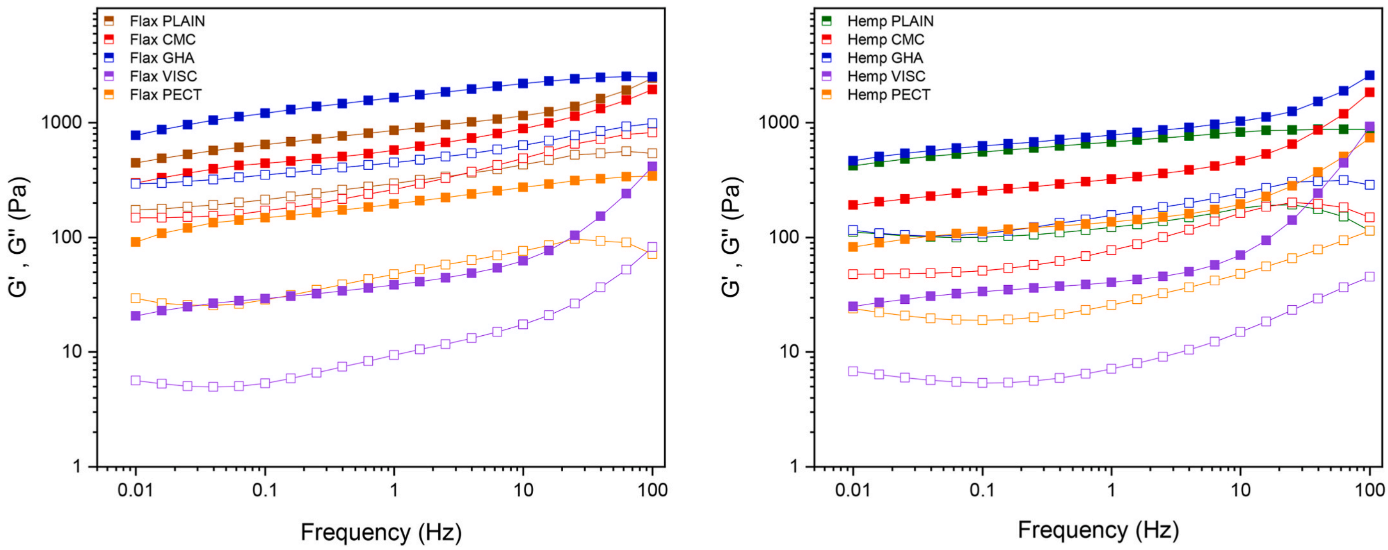

Fig. 4. Mechanical spectra of flaxseed-based (left) and hempseed-based (right) purees. Storage (G′) and loss (G") moduli are shown with filled and open markers, respectively.

in back extrusion results, confirms GHA's ability to enhance network connectivity through hydrogen bonding and polymer chain entanglement (Morris et al., 2012). The resulting matrix exhibits increased resistance at rest while preserving controlled deformability under shear. CMC produced a milder reinforcement effect, consistent with its mechanism based primarily on polymer-solvent interactions rather than extensive network formation (Gupta et al., 2021). Enzymatic treatments substantially reduced viscoelastic parameters, confirming matrix weakening due to polysaccharide hydrolysis and consequent disruption of network organization.

To quantitatively characterize network architecture and interaction strength, viscoelastic data were analyzed using Bohlin's weak gel model, a validated approach for soft-solid foods. The model was applied to the mechanical spectra according to Eq. (8) (Gabriele et al., 2001):

$$G^* = \sqrt{G'^2 + G''^2} = A_f \omega^{1/z} \quad (8)$$

In this framework, the coordination number Z (dimensionless) describes network connectivity, that is the effective number of rheological units interacting within the three-dimensional structure, while A_f (Pa·s$^{1/z}$) reflects gel strength and the overall interaction intensity between structural units, and ω is the angular frequency (rad/s). Together, these parameters describe both structural organization and mechanical robustness. While yield stress indicates the onset of macroscopic flow, Bohlin parameters quantify mesoscopic network connectivity, enabling differentiation between formulations with similar viscosity but distinct structural organization.

Flax-based formulations consistently exhibited higher Z and A_f values than hemp-based ones (Table 9), indicating more interconnected and mechanically stable networks, as predicted by the relation $G^* \propto \omega^{1/z}$ (Bohlin, 1980). These results quantitatively confirm the ability of flax-derived polysaccharides to generate extended three-dimensional structures through multiple interaction mechanisms (Troshchynska et al., 2022).

The additive effects of viscosity-modulators followed a clear hierarchy. GHA yielded the highest Z and A_f values across both protein matrices, demonstrating its capacity to reinforce interparticle connectivity even at low concentrations (Torres et al., 2019). CMC slightly increased Z but reduced A_f, reflecting modest structural organization without substantial strengthening. Conversely, enzymatic treatments markedly decreased both parameters – particularly in VISC-modified samples – quantifying the extent of network degradation.

Overall, dynamic rheology and mechanical analyses indicate that microstructural modulation – through protein source, hydrocolloid incorporation, or enzymatic treatment – governs bulk resistance, deformability, and interfacial interactions. The agreement between Bohlin parameters, back extrusion data, and mucoadhesion measurements highlights the strong coupling between mesoscopic organization and macroscopic texture.

From a functional perspective, formulations with higher network coordination and moderate gel strength showed improved structural integrity during deformation while maintaining controlled flow under shear. This balance is critical in texture-modified foods, where excessive rigidity may hinder deformation and insufficient cohesion may compromise bolus stability.

The combined use of rheology, back extrusion, and mucoadhesion provides an integrated framework linking structure to mechanical and interfacial performance during oral processing. This approach supports the rational tuning of texture within IDDSI consistency ranges, grounding formulation design in measurable physical parameters rather than purely empirical classification.

Table 9
Weak-gel model parameters obtained from mechanical spectra.

	Flax-based					Hemp-based				
	PLAIN	CMC	GHA	VISC	PECT	PLAIN	CMC	GHA	VISC	PECT
A_f (Pa·s$^{1/z}$)	660	447	1354	22	106	521	247	635	17	70
Z (–)	7.05	7.16	9.02	2.80	2.97	6.88	7.03	8.75	2.07	2.74

Af: gel strength; Z: coordination number; CMC: carboxymethylcellulose; GHA: high-acyl gellan gum; VISC: viscozyme; PECT: pectinase.

3.6. Tribology: an interfacial complement

Tribological testing provides a critical interfacial complement to bulk rheological and mechanical analyses in characterizing texture-modified soft-solid systems. While rheology and back extrusion describe bulk viscoelastic resistance and structural integrity, tribology captures the frictional behavior at the interface between the food matrix and oral surfaces during dynamic deformation. These interfacial properties strongly influence lubrication, perceived smoothness, and resistance to bolus movement (Xu et al., 2022).

Within a multiscale framework, tribology extends structural interpretation from internal network organization to surface-mediated interactions. The Stribeck curve provides the theoretical basis for analyzing these phenomena, identifying three lubrication regimes – boundary, mixed, and hydrodynamic – that reflect progressive surface separation under increasing sliding speed (Sarkar et al., 2021).

All puree formulations exhibited characteristic Stribeck profiles (Fig. 5), confirming the presence of the three lubrication regimes. At low sliding speeds ($< 10^{-3}$ m/s), the friction coefficient (μ) increased sharply, indicating boundary lubrication dominated by direct asperity contact and thin lubrication films. As speed increased, μ decreased marking the transition to the mixed regime, where partial surface separation occurs and the sample begins to function as an effective lubricant. At higher velocities ($> 5 \cdot 10^{-1}$ m/s), a slight increase in μ was observed, corresponding to the hydrodynamic regime, where viscous drag predominates and a continuous fluid film separates the interacting surfaces.

This well-defined transition demonstrates the ability of the formulated purees to adapt frictionally to increasing shear conditions. Such adaptability is particularly relevant for soft-solid foods, where controlled lubrication is required to balance structural cohesion with smooth interfacial flow.

Formulation variables significantly influenced tribological response. The incorporation of structuring agents increased friction coefficients, particularly in the boundary and mixed regimes. GHA consistently produced the highest μ values, followed by CMC, while PLAIN and enzymatically treated formulations exhibited markedly lower friction. The elevated friction observed in GHA-enriched samples is consistent with its strong gel-forming capacity and the formation of entangled polymeric networks resistant to shear-induced thinning (Gomes et al., 2023). CMC-treated purees displayed intermediate frictional behavior, reflecting its thickening mechanism based primarily on chain entanglement and electrostatic interactions rather than extensive three-dimensional network formation (Lopez et al., 2015).

Conversely, enzymatically treated purees showed substantially reduced friction coefficients across all regimes. Enzymatic depolymerization disrupts structural polysaccharides and weakens intermolecular interactions, producing systems with reduced internal cohesion and enhanced lubrication (Hu et al., 2021).

These interfacial differences are closely consistent with the rheological, back extrusion, and mucoadhesion findings. Formulations with higher yield stress, greater extrusion forces, and stronger mucoadhesive interactions also showed higher friction coefficients, indicating that tribological behavior reflects both bulk structural resistance and surface-associated mechanisms, such as polymer adsorption and interfacial network rearrangement.

From a functional perspective, higher-friction systems provide greater resistance to interfacial slip and may support more controlled bolus deformation, whereas lower-friction systems facilitate smoother sliding and reduced interfacial drag. Excessively high friction may increase perceived resistance during oral manipulation, while excessively low friction may reduce structural control. Therefore, optimizing frictional properties must be considered alongside bulk viscoelastic parameters to achieve balanced texture performance.

Taken together, tribological assessment completes the multiscale characterization of the formulated purees by integrating surface lubrication behavior with internal structural organization. The formulation-dependent modulation of lubrication regimes shows that frictional performance is not solely driven by viscosity but is governed by coordinated bulk-interface interactions. This interdependence underscores the importance of incorporating tribology into the rational design of texture-modified soft-solid foods, enabling precise tuning of interfacial dynamics alongside rheological and mechanical properties. Future studies may further refine tribological benchmarks for structured soft-solids by defining frictional and interfacial reference ranges across viscosity-based texture classes. Integrating tribological data with rheological, mucoadhesive, and mechanical measurements provides a robust framework for understanding how formulation variables modulate coupled bulk and interfacial behavior. This approach supports rational, quantitatively guided formulation of texture-controlled food systems.

4. Conclusions

Conventional characterization of plant protein soft-solids often relies on bulk viscosity and yield stress, which do not fully capture formulation effects on lubrication and interfacial behavior during oral processing.

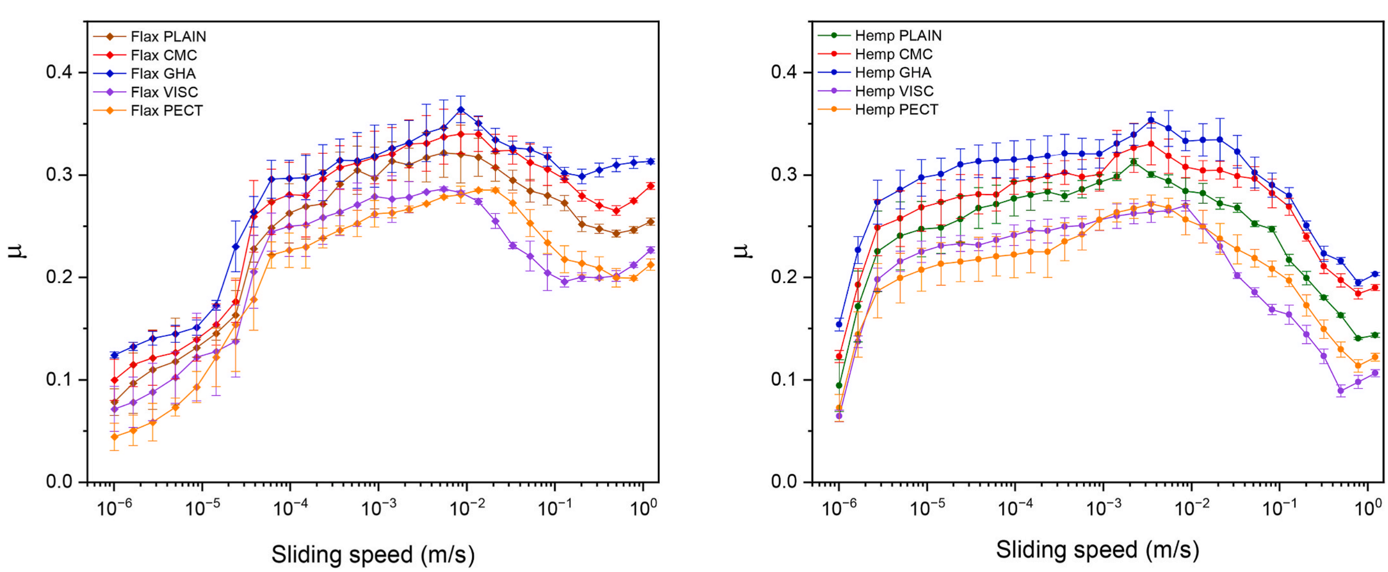

Fig. 5. Stribeck curves of flaxseed-based (left) and hempseed-based (right) purees.

This study addressed this limitation by investigating zucchini-based soft-solid systems formulated under realistic compositional constraints, targeting both a “high in protein” claim and reduced sodium content.

The comparative analysis showed that protein source and the incorporation of structuring (hydrocolloids) or destructuring (enzymatic) agents significantly influence oral processing-relevant properties. Hydrocolloids primarily governed low-shear stability, lubrication, and interfacial retention, whereas protein source and enzymatic treatments modulated network strength and structural recovery. Among the tested systems, flaxseed protein combined with high-acyl gellan gum provided the most balanced mechanical and interfacial performance.

Overall, these findings demonstrate how formulation design, under nutritionally relevant constraints, governs oral behavior in plant-based soft-solids, providing a practical basis for texture-controlled product development. This work bridges formulation-driven design with oral-processing functionality in plant-based soft-solids.

CRediT authorship contribution statement

Laura Piazza: Writing – review & editing, Writing – original draft, Validation, Supervision, Resources, Project administration, Funding acquisition, Conceptualization. **Giorgio Innocenzo Ascrizzi:** Writing – review & editing, Visualization, Software, Methodology, Investigation, Formal analysis, Data curation.

Declaration of AI-assisted technologies

The authors acknowledge the use of artificial intelligence tools (ChatGPT and InstaText) solely for grammar improvement and editorial refinement. After using these tools, the authors reviewed and edited the content as needed and take full responsibility for the published article. All scientific content, including the design, data analysis, interpretation, and conclusions, was developed entirely by the authors, without assistance of AI tools in the research process.

Fundings

The study was funded under the National Recovery and Resilience Plan (NRRP), Mission 4 Component 2 Investment 1.3 - Call for proposals No. 341 of 15 March 2022 of Italian Ministry of University and Research funded by the European Union-NextGenerationEU, Award Number: Project code PE00000003, Concession Decree No. 1550 of 11 October 2022 adopted by the Italian Ministry of University and Research, CUP D93C22000890001, Project title “ON Foods - Research and innovation network on food and nutrition Sustainability, Safety and Security - Working ON Foods”. The authors acknowledge support from the University of Milan through the APC initiative.

Declaration of competing interest

The authors declare that they have no known competing financial interests or personal relationships that could have appeared to influence the work reported in this paper.

Acknowledgments

The authors wish to thank Prof. *Simone Stella* (Department of Veterinary Medicine and Animal Sciences, University of Milan) for his assistance in retrieving of porcine oral mucosae used in the study.

The authors wish to thank Dr. *Nicolò Pestarino* for his technical assistance and dedicated support during the experimental phase.

Appendix A. Supplementary data

Supplementary data to this article can be found online at https://doi.org/10.1016/j.lwt.2026.119443.

Data availability

Data will be made available on request.

References

Alfaro-Rodríguez, M.-C., García, M. C., Prieto-Vargas, P., & Muñoz, J. (2024). Rheological properties and physical stability of aqueous dispersions of flaxseed fibers. *Gels, 10*(12), 787. https://doi.org/10.3390/gels10120787

Ascrizzi, G. I., & Piazza, L. (2025). Oral textural properties of easy-to-swallow foods. *Chemical Engineering Transactions, 118*, 37–42. https://doi.org/10.3303/CET25118007

Association of Official Analytical Chemist (AOAC). (2023). In *Official methods of analysis of AOAC international. 22nd edition*. Rockville: AOAC International.

Baixauli, R., Bolivar-Prados, M., Ismael-Mohammed, K., Clavé, P., Tárrega, A., & Laguna, L. (2022). Characterization of dysphagia thickeners using texture analysis—What information can be useful? *Gels, 8*(7). https://doi.org/10.3390/gels8070430

Bassi da Silva, J., Ferreira, S. B. de S., de Freitas, O., & Bruschi, M. L. (2017). A critical review about methodologies for the analysis of mucoadhesive properties of drug delivery systems. *Drug Development and Industrial Pharmacy, 43*(7), 1053–1070. https://doi.org/10.1080/03639045.2017.1294600

Bayer, I. S. (2022). Recent advances in mucoadhesive interface materials, mucoadhesion characterization, and technologies. *Advanced Materials Interfaces, 9*(18). https://doi.org/10.1002/admi.202200211

Bohlin, L. (1980). A theory of flow as a cooperative phenomenon. *Journal of Colloid and Interface Science, 74*(2), 423–434. https://doi.org/10.1016/0021-9797(80)90211-8

Bolivar-Prados, M., Tomsen, N., Hayakawa, Y., Kawakami, S., Miyaji, K., Kayashita, J., & Clavé, P. (2022). Proposal for a standard protocol to assess the rheological behavior of thickening products for oropharyngeal dysphagia. *Nutrients, 14*(23). https://doi.org/10.3390/nu14235028

Carvalho, F. C., Bruschi, M. L., Evangelista, R. C., & Gremião, M. P. D. (2010). Mucoadhesive drug delivery systems. *Brazilian Journal of Pharmaceutical Sciences, 46*(1), 1–17. https://doi.org/10.1590/S1984-82502010000100002

Chen, H., Xu, B., Wang, Y., Li, W., He, D., Zhang, Y., Zhang, X., & Xing, X. (2023). Emerging natural hemp seed proteins and their functions for nutraceutical applications. *Food Science and Human Wellness, 12*(4), 929–941. https://doi.org/10.1016/j.fshw.2022.10.016

Chen, Y., Zhu, H., Feng, Y., Wang, Y., Wang, X., Zhang, W., & Luo, Y. (2026). Rheological analysis in food processing: Factors, applications, and future outlooks with machine learning integration. *RSC Advances, 16*(6), 5040–5063. https://doi.org/10.1039/D5RA07499A

Cichero, J. A. Y., Lam, P., Steele, C. M., Hanson, B., Chen, J., Dantas, R. O., Duivestein, J., Kayashita, J., Lecko, C., Murray, J., Pillay, M., Riquelme, L., & Stanschus, S. (2017). Development of international terminology and definitions for texture-modified foods and thickened fluids used in dysphagia management: The IDDSI framework. *Dysphagia, 32*(2), 293–314. https://doi.org/10.1007/s00455-016-9758-y

Cook, S. L., Bull, S. P., Methven, L., Parker, J. K., & Khutoryanskiy, V. V. (2017). Mucoadhesion: A food perspective. *Food Hydrocolloids, 72*, 281–296. https://doi.org/10.1016/j.foodhyd.2017.05.043

Cuomo, F., Angelicola, M., De Arcangelis, E., Lopez, F., Messia, M. C., & Marconi, E. (2021). Rheological and nutritional assessment of dysphagia-oriented new food preparations. *Foods, 10*(3), 663. https://doi.org/10.3390/foods10030663

da Silva, G. M., da Rocha, R. F. P., da Costa, M. P. M., Ferreira, I. L. de M., & Delpech, M. C. (2018). Evaluation of viscometric properties of carboxymethylcellulose and gellan. *Journal of Molecular Liquids, 268*, 201–205. https://doi.org/10.1016/j.molliq.2018.07.062

de Araújo, J. S. M., Volpato, M. C., Muniz, B. V., Xavier, G. G. A., Martinelli, C. C. M., Lopez, R. F. V., Groppo, F. C., & Franz-Montan, M. (2021). Resistivity technique for the evaluation of the integrity of buccal and esophageal epithelium mucosa for *in vitro* permeation studies: Swine buccal and esophageal mucosa barrier models. *Pharmaceutics, 13*(5), 643. https://doi.org/10.3390/pharmaceutics13050643

Dhamodharan, G., Cox, A., Makame, J., & Nolden, A. A. (2025). Sensory implications of thickened beverages for dysphagia: Taste-texture interactions. *LWT – Food Science and Technology, 225*, Article 117880. https://doi.org/10.1016/j.lwt.2025.117880

Douglas, J. (2018). Weak and strong gels and the emergence of the amorphous solid state. *Gels, 4*(1), 19. https://doi.org/10.3390/gels4010019

Gabriele, D., de Cindio, B., & D'Antona, P. (2001). A weak gel model for foods. *Rheologica Acta, 40*, 120–127. https://doi.org/10.1007/s003970000139

Gao, Y., Liu, R., & Liang, H. (2024). Food hydrocolloids: Structure, properties, and applications. *Foods, 13*(7), 1077. https://doi.org/10.3390/foods13071077

Garcia-Tarazona, Y. M., Morantes, S. J., Gordillo, J. F. I., Sepúlveda, P., Ramos, F. A., & Lafaurie, G. I. (2023). Candesartan exhibits low intrinsic permeation capacity and affects buccal tissue viability and integrity: An ex vivo study in porcine buccal mucosa. *European Journal of Pharmaceutical Sciences, 188*, Article 106495. https://doi.org/10.1016/j.ejps.2023.106495

Giura, L., Urtasun, L., Belarra, A., Ansorena, D., & Astiasarán, I. (2021). Exploring tools for designing dysphagia-friendly foods: A review. *Foods, 10*(6), 1334. https://doi.org/10.3390/foods10061334

Gomes, D., Batista-Silva, J. P., Sousa, A., & Passarinha, L. A. (2023). Progress and opportunities in gellan gum-based materials: A review of preparation, characterization and emerging applications. *Carbohydrate Polymers, 311*, Article 120782. https://doi.org/10.1016/j.carbpol.2023.120782

Gupta, B., Mishra, V., Gharat, S., Momin, M., & Omri, A. (2021). Cellulosic polymers for enhancing drug bioavailability in ocular drug delivery systems. *Pharmaceuticals, 14* (11), 1201. https://doi.org/10.3390/ph14111201

Hadnađev, M., Dapčević-Hadnađev, T., Lazaridou, A., Moschakis, T., Michaelidou, A.-M., Popović, S., & Biliaderis, C. G. (2018). Hempseed meal protein isolates prepared by different isolation techniques. Part I. Physicochemical properties. *Food Hydrocolloids, 79*, 526–533. https://doi.org/10.1016/j.foodhyd.2017.12.015

Hu, T.-G., Zou, Y.-X., Li, E.-N., Liao, S.-T., Wu, H., & Wen, P. (2021). Effects of enzymatic hydrolysis on the structural, rheological, and functional properties of mulberry leaf polysaccharide. *Food Chemistry, 355*, Article 129608. https://doi.org/10.1016/j.foodchem.2021.129608

Huang, Y., Takhar, P. S., Tang, J., & Swanson, B. G. (2008). Flow behaviors of high acyl gellan aqueous solutions as affected by temperature, and calcium and gellan concentrations. *International Journal of Food Engineering, 4*(5). https://doi.org/10.2202/1556-3758.1279

Ibañez, F. C., Merino, G., Marín-Arroyo, M. R., & Beriain, M. J. (2022). Instrumental and sensory techniques to characterize the texture of foods suitable for dysphagic people: A systematic review. *Comprehensive Reviews in Food Science and Food Safety, 21*(3), 2738–2771. https://doi.org/10.1111/1541-4337.12957

Julakanti, S., Charles, A. P. R., Syed, R., Bullock, F., & Wu, Y. (2023). Hempseed polysaccharide (*Cannabis sativa L.*): Physicochemical characterization and comparison with flaxseed polysaccharide. *Food Hydrocolloids, 143*, Article 108900. https://doi.org/10.1016/j.foodhyd.2023.108900

Karabulut, G., Kahraman, O., Pandalaneni, K., Kapoor, R., & Feng, H. (2023). A comprehensive review on hempseed protein: Production, functional and nutritional properties, novel modification methods, applications, and limitations. *International Journal of Biological Macromolecules, 253*, Article 127240. https://doi.org/10.1016/j.ijbiomac.2023.127240

Kučka, M., Harenčár, Ľ., Ražná, K., Nôžková, J., Kowalczewski, P.Ł., Deyholos, M., Dziedzic, K., Rybicka, I., Zembrzuska, J., Kačániová, M., Ivanišová, E., Gažo, J., Čerteková, S., & Tomka, M. (2024). Great potential of flaxseed mucilage. *European Food Research and Technology, 250*(3), 877–893. https://doi.org/10.1007/s00217-023-04429-0

Lee, S. Y., Chung, S.-J., Lim, J.-W., Kim, M. Y., & Ha, C. H. (2025). Texture characterization of semi-solid foods for older adults: Sensory analysis and instrumental approaches. *LWT – Food Science and Technology, 221*, Article 117582. https://doi.org/10.1016/j.lwt.2025.117582

Lopez, C. G., Rogers, S. E., Colby, R. H., Graham, P., & Cabral, J. T. (2015). Structure of sodium carboxymethyl cellulose aqueous solutions: A SANS and rheology study. *Journal of Polymer Science Part B: Polymer Physics, 53*(7), 492–501. https://doi.org/10.1002/polb.23657

Lorenc, F., Jarošová, M., Bedrníček, J., Smetana, P., & Bárta, J. (2022). Structural characterization and functional properties of flaxseed hydrocolloids and their application. *Foods, 11*(15), 2304. https://doi.org/10.3390/foods11152304

Machado, M., Costa, E. M. A. da, & Silva, S. (2025). Soft gels in food systems: Recent advances, applications, and technological innovations. *Gels, 11*(8), 667. https://doi.org/10.3390/gels11080667

Mendoza-Pérez, R. J., Náthia-Neves, G., Blanco, B., Vela, A. J., Caballero, P. A., & Ronda, F. (2024). Physicochemical characterisation of seeds, oil and defatted cake of three hempseed varieties cultivated in Spain. *Foods, 13*(4), 531. https://doi.org/10.3390/foods13040531

Michaelis, J. U., Kiese, S., Amann, T., Folland, C., Asam, T., & Eisner, P. (2023). Thickening properties of carboxymethyl cellulose in aqueous lubrication. *Lubricants, 11*(3). https://doi.org/10.3390/lubricants11030112

Morris, E. R., Nishinari, K., & Rinaudo, M. (2012). Gelation of gellan – A review. *Food Hydrocolloids, 28*(2), 373–411. https://doi.org/10.1016/j.foodhyd.2012.01.004

Nishinari, K., Ishihara, S., Hori, K., & Fang, Y. (2020). Tongue-palate squeezing of soft gels in food oral processing. *Trends in Food Science & Technology, 99*, 117–132. https://doi.org/10.1016/j.tifs.2020.02.023

Perrot, A., Mélinge, Y., Estellé, P., Rangeard, D., & Lanos, C. (2011). The back extrusion test as a technique for determining the rheological and tribological behaviour of yield stress fluids at low shear rates. *Applied Rheology, 21*(5). https://doi.org/10.3933/ApplRheol-21-53642

Pestana, A. M., Calixto, G. M. F., Bezerra, A. A. C., de Morais Ribeiro, L. N., da Costa, A. C., Moraes, Â. M., & Franz-Montan, M. (2024). Analysis of key factors for evaluating mucosal adhesion using swine buccal tissue. *Journal of Pharmaceutical Sciences, 113*(8), 2413–2419. https://doi.org/10.1016/j.xphs.2024.04.018

Piazza, L., Esposito, M., & Masseroni, E. (2023). Upcycling pears with physiopathy into soft solid foods intended for people with swallowing difficulties: Formulation, rheology and tribology studies. *Chemical Engineering Transactions, 102*, 181–186. https://doi.org/10.3303/CET23102031

Principato, L., Carullo, D., Gruppi, A., Lambri, M., Bassani, A., & Spigno, G. (2024). Correlation of rheology and oral tribology with sensory perception of commercial hazelnut and cocoa-based spreads. *Journal of Texture Studies, 55*(4). https://doi.org/10.1111/jtxs.12850

Ross, A. I. V., Tyler, P., Borgognone, M. G., & Eriksen, B. M. (2019). Relationships between shear rheology and sensory attributes of hydrocolloid-thickened fluids designed to compensate for impairments in oral manipulation and swallowing. *Journal of Food Engineering, 263*, 123–131. https://doi.org/10.1016/j.jfoodeng.2019.05.040

Sarkar, A., Soltanahmadi, S., Chen, J., & Stokes, J. R. (2021). Oral tribology: Providing insight into oral processing of food colloids. *Food Hydrocolloids, 117*, Article 106635. https://doi.org/10.1016/j.foodhyd.2021.106635

Thirawong, N., Nunthanid, J., Puttipipatkhachorn, S., & Sriamornsak, P. (2007). Mucoadhesive properties of various pectins on gastrointestinal mucosa: An *in vitro* evaluation using texture analyzer. *European Journal of Pharmaceutics and Biopharmaceutics, 67*(1), 132–140. https://doi.org/10.1016/j.ejpb.2007.01.010

Torres, O., Yamada, A., Rigby, N. M., Hanawa, T., Kawano, Y., & Sarkar, A. (2019). Gellan gum: A new member in the dysphagia thickener family. *Biotribology, 17*, 8–18. https://doi.org/10.1016/j.biotri.2019.02.002

Troshchynska, Y., Bleha, R., Synytsya, A., & Štětina, J. (2022). Chemical composition and rheological properties of seed mucilages of various yellow- and brown-seeded flax (*Linum usitatissimum L.*) cultivars. *Polymers, 14*(10), 2040. https://doi.org/10.3390/polym14102040

World Health Organization. (2023). WHO global report on sodium intake reduction. https://iris.who.int/handle/10665/366393.

Xu, W., Yu, S., & Zhong, M. (2022). A review on food oral tribology. *Friction, 10*(12), 1927–1966. https://doi.org/10.1007/s40544-022-0594-9